

## Mechanism of Damnacanthal Induced Apoptosis in CEM-SS Cell Line

(Mekanisme Apoptosis Teraruh Damnacanthal dalam Titisan Sel CEM-SS)

BANULATA GOPALSAMY, SAIFUL YAZAN LATIFAH\* & HISYAM ABDUL HAMID

*Department of Biomedical Science, Faculty of Medicine and Health Sciences, Universiti Putra Malaysia, 43400 UPM Serdang, Selangor, Malaysia*

*Received: 9 January 2024/Accepted: 5 August 2024*

### ABSTRACT

Leukaemia, is cancer of organs that is responsible to produce blood specifically the lymphatic system and bone marrow. Due to the harsh effects of currently used cancer drugs, damnacanthal, an anthraquinone obtained from the roots of *Morinda elliptica* is tested as a potential anticancer agent. This study reports on the participation of the p53, Bcl-2 and Bax in the apoptosis induced by of damnacanthal, on T-lymphoblastic leukaemia (CEM-SS) cell. Cell viability and morphology was tested with trypan blue assay, flow cytometry analysis detected the apoptotic activity of damnacanthal, caspase colorimetric protease assay tested the Caspase 2, 3, 6, 8, and 9's involvement and Enzyme-linked Immunosorbent Assay (ELISA) was carried out to quantify the Human p53, Bcl-2, and Bax expression levels. Damnacanthal exhibited cytotoxicity at doses 10 and 30 µg/mL after 72 h of incubation. This study reports that damnacanthal arrested the cell at G2/M phase and initiates the apoptotic activity in the cells treated with 30 µg/mL of damnacanthal for 72 h through caspase 2 and 6 activation and not caspases 3, 8, and 9. Furthermore, this anthraquinone induces apoptosis via p53-independent pathway. Damnacanthal also lowered Bcl-2 and increased Bax activity in CEM-SS cell lines. These anticancer properties of damnacanthal makes it a potential agent to treat T-lymphoblastic leukaemia.

Keywords: Anticancer; apoptosis; CEM-SS; damnacanthal

### ABSTRAK

Leukemia adalah kanser bagi organ yang bertanggung jawab menghasilkan darah, terutamanya sistem limfa dan sum sum tulang. Disebabkan kesan yang buruk oleh ubat kanser yang sedia ada, damnacanthal, salah satu antrakuinon yang diperoleh daripada akar *Morinda elliptica* telah diuji sebagai agen anti kanser yang berpotensi. Penyelidikan ini melaporkan penglibatan p53, Bcl-2 dan Bax dalam apoptosis aruhan damnacanthal, ke atas sel T-limfoblastik leukemia (CEM-SS). Kemandirian sel dan morfologi telah diuji dengan ujian tripan biru, analisis sitometri aliran mengesan aktiviti apoptosis damnacanthal, ujian protease kolorimetrik caspase menguji penglibatan Caspase 2, 3, 6, 8 dan 9 dan Ujian Imunosorben Berkaitan Enzim (ELISA) telah dijalankan untuk mengukur tahap pengekspresan p53, Bcl-2 dan Bax manusia. Damnacanthal menunjukkan sitotoksiti pada dos 10 dan 30 µg/mL selepas 72 jam pengeraman. Kajian ini melaporkan bahawa damnacanthal menahan sel pada fasa G2/M dan memulakan aktiviti apoptosis dalam sel yang dirawat dengan 30 µg/mL damnacanthal selama 72 jam melalui pengaktifan caspase 2 dan 6 dan bukan caspases 3, 8 dan 9. Tambahan pula, antrakuinon ini mendorong apoptosis melalui laluan bebas p53. Damnacanthal juga menurunkan Bcl-2 dan meningkatkan aktiviti Bax dalam sel CEM-SS. Sifat antikanser damnacanthal ini menjadikannya agen berpotensi untuk merawat leukemia T-limfoblastik.

Kata kunci: Antikanser; apoptosis; CEM-SS; damnacanthal

### INTRODUCTION

Cancer is defined as an uncontrollable, rapid division of cells that have undergone mutations to their DNA within the cells, making them abnormal. These cancer cells eventually infiltrate into normal body tissues. The human

body's usual function is interfered due to the chemicals produced by the cancer cells. It is projected that in US alone in the year 2023, the total number of new cancer cases to be 1, 958, 310 whereby 609,820 cases lead to mortality (Siegel et al. 2023).

Based on the most recent cancer cases reports in Malaysia, 48,639 new cases with 29,530 mortalities were reported in the year 2020 (GLOBOCAN 2020). Leukaemia being the 9<sup>th</sup> most common cancer in Malaysia, recorded 1 905 cases accounting for 3.9% of all types of cancers and 1,481 number of deaths (GLOBOCAN 2020). As of 2019, leukaemia is the commonest cause of death and disability-adjusted life years among the cancer driven children of both genders and age groups worldwide.

Leukaemia is one of the few commonest diagnosed cancers among children (WHO 2021). To date, most cancer cases are still alarming despite the latest drug therapies, treatment with radiation and chemotherapy. Nausea, exhaustion, constipation, hair loss, diarrhoea, vomiting, fever, mouth sore, muscular, and other pains and weaknesses are among the adverse side effects of the treatments (Anand et al. 2022; Katta et al. 2023).

Newer treatment alternatives are constantly considered to address the undesired side effects of cancer treatments. Natural products are among the most sought after to be used in medicinal practice and is highly preferred by healthcare providers and the general public. To date, scientists are researching the major beneficial constituent present in plants to be tested out for its possible anticancer properties. *Morinda elliptica*, generally recognised as 'mengkudu kecil' by the locals, is widely applied in traditional folk medicine to improve appetite, treat diarrhea, cholera, headache, and piles (Chong et al. 2005). Nor Hadiani et al. (1997) documented that damnacanthal, is one of the 11 anthraquinones successfully isolated from *M. elliptica*. This anthraquinone has been documented for its many medical benefits such as improved immunity (Hirazumi et al. 1996), antioxidant (Ismail et al. 2002) and antibacterial (Shami 2018) properties.

Interestingly, damnacanthal exhibited antitumour and anticancer properties across numerous cancer cell types, such as Hep G2 human hepatocellular carcinoma cells (García-Vilas, Quesadal & Medina 2015) and oral squamous cell carcinoma cells (Shaghayegh et al. 2017). Damnacanthal caused a cell cycle arrest at G1 checkpoint, and induced p53-mediated apoptosis through the activation of p21 and caspase 7 in MCF-7 breast cancer (Aziz et al. 2014). Damnacanthal suppressed colorectal tumorigenesis by enhancing the transcriptional factor CCAAT/enhancer binding protein  $\beta$  (C/EBP $\beta$ ) which in turn induced nonsteroidal anti-inflammatory activated gene-1 (NAG1), a proapoptotic protein (Nuansanit et al. 2012) and also downregulate the cell cycle protein cyclin D1 (Woradulayapinij et al. 2022). Damnacanthal also inhibited the growth of ovarian cancer via the ERK/mTOR/autophagy signaling cascade (Li et al. 2022).

In CEM-SS cells however, damnacanthal exerted a growth inhibitory response by apoptosis and necrosis (Latifah et al. 2022). It induced condensation and fragmentation of the nuclear chromatin, further causing fragmentation of the cytoplasm and nuclei by activating the Mg<sup>2+</sup>/Ca<sup>2+</sup>-dependent endonuclease. The plasma membrane and cytoskeleton of the CEM-SS cells underwent morphological changes and the microvilli disappeared indicating apoptosis of the cell (Latifah et al. 2022). Furthermore, damnacanthal exerted a cytostatic effect by inducing a G0/G1 phase cell cycle arrest (Latifah et al. 2021) inhibiting the growth of CEM-SS cells.

p53 is a transcription factor present in the cell nucleus and cytoplasm that binds specifically to anti-apoptotic proteins, Bcl-2. p53 leads to the desensitization the cells from the apoptotic stimuli, which lowers the Bcl-2 levels indirectly inducing apoptosis (Wei et al. 2021). p53 also initiates apoptosis by activating the pro-apoptotic protein Bax or by disrupting the Bax complex (Chipuk et al. 2004; Wang et al. 2023).

Caspase 2, 8, and 9 are known as initiator caspases, whereby they are activated by pro-apoptotic signals. These caspases in turn cleave and leads to the activation of Caspase 3 and 6, also known as the effector caspases (Green et al. 2022; Hounsell & Fan 2021). These caspases have unique roles as tumor suppressors in various tissue types (Silva et al. 2019).

Even though the apoptotic activity of damnacanthal is evident, the specific mechanism that is involved needs to be elucidated. Therefore, this study investigated the p53, Bcl-2, and Bax expression levels. Here, we report the roles of caspases 2, 3, 6, 8, and 9 in damnacanthal's apoptotic activity in CEM-SS cell line.

## MATERIALS AND METHODS

### COMPOUND

Damnacanthal was extracted from *Morinda elliptica*. The extraction method is as specified by Latifah et al. (2022, 2021). The compound was provided by Prof. Dr. Nordin Lajis from Universiti Putra Malaysia. Damnacanthal was prepared by dissolving it in DMSO.

### CELLS

The human acute T-lymphoblastic leukaemia cell line (CEM-SS) was attained from the National Cancer Institute (NCI), USA. The cells were grown in RPMI 1640 supplemented with 10% of fetal bovine serum (PAA, Austria) and 1% of antibiotics (100 units/mL penicillin and 100  $\mu$ g/mL streptomycin) at 37 °C under 5% CO<sub>2</sub> in a humidified atmosphere.

#### TREATMENT

The CEM-SS cells at initial concentration of  $1 \times 10^6$  cells/mL were treated with 1, 3, 10 and 30  $\mu\text{g/mL}$  of damnacanthal and control, without the compound was included. The cells were incubated in their respective treatments for periods of 24, 48, and 72 h. The observations were carried out by a team of investigators. Each treatment was given a code number blinded from the investigator from knowing which treatment is given to a particular sample to avoid bias.

#### CELL VIABILITY

The cells treated with damnacanthal and control cells underwent an incubation period of 72 h, and was sampled for every 24 h. The cells were stained with 0.25% trypan blue and the cell count and viability were calculated by using haemocytometer under a light microscope. Cells that absorbed the blue coloration were considered dead while clear appearing cells were counted as cells that are still viable. The viability percentage against the treatment graph was plotted.

#### MORPHOLOGICAL CHANGES

Any changes to the cell morphology, specifically the presence of apoptotic and necrotic features in the cells treated with damnacanthal (1, 3, 10, and 30  $\mu\text{g/mL}$ ) and the control group for 24, 48, and 72 h were identified under an inverted light microscope (Olympus, USA) at 400X magnification.

#### ANALYSIS OF CELL CYCLE

Cells at a concentration of  $1 \times 10^6$  cells/mL were treated with 1, 3, 10, and 30  $\mu\text{g/mL}$  of damnacanthal and untreated control, incubated for 24, 48, and 72 h were collected for cell cycle analysis. The cells were centrifuged at 1000 rpm for 10 min and rinsed with phosphate buffered saline. The cells were then fixed for flow cytometry analyses according to Klucar and al-Rubeai (1997). Briefly, 50% cold ethanol was used to fix the cell pellets and kept at 4 °C for 15 min. Cells were then spun at 1000 rpm for 10 min, before the cell pellet was resuspended for 20 min in a solution containing 0.425 mL of PBS, 25  $\mu\text{L}$  of propidium iodide (1 mg/mL) and 50  $\mu\text{L}$  of RNase A (1 mg/mL). The cell cycle profile was analyzed using flow cytometry machine (FACSCalibur flow cytometer, Becton Dickinson, USA) with CellQuest software.

#### CASPASE 2, 3, 6, 8, AND 9 ACTIVITY

ApoTarget™ Caspase Colorimetric Protease Assay from Invitrogen™ (BioSource, CA) was used to determine the activities of Caspase 2, 3, 6, 8, and 9.

After incubation periods of 24 and 72 h, the cells were spun at 1000 rpm for 10 min. Fifty microlitre of chilled cell lysis buffer was mixed into the cells and kept chill for 10 min. The cells were then spun for 1 min at 14,000 rpm. The supernatant was subjected to Bradford assay to analyse the protein content of the samples. The extract was diluted as such where each 50  $\mu\text{L}$  cell lysis buffer contained 50-200  $\mu\text{g}$  protein. Fifty microlitre of 2x reaction buffer containing 10 mM DTT was pipetted into the samples. Five microlitre of the 4 mM substrate was pipetted into the sample wells and kept at 37 °C away from light for 2 h. The plate was read by using an ELISA microplate reader (Sunrise, Tecan, Austria) with Magellan software at 405 nm.

#### P53 PROTEIN LEVELS

##### PREPARATION OF CELL LYSATE

For the preparation and detection procedure in determining the level of p53, the Human p53 ELISA Kit from Bendermed Systems (Austria) was used. The treated (1, 2, 10, and 30  $\mu\text{g/mL}$ ) and untreated cells (control) collected after 24, 48, and 72 h of incubation, were spun at 1200 rpm ( $300 \times g$ ) for 5 min. The pellet was washed a few times before 200  $\mu\text{L}$  of cell extraction buffer with 1% protease inhibitor cocktail was pipetted into the pellet (cells), vortexed for 10 min and kept chill for 10 min. The mixture was again centrifuged at 1400 rpm for 10 min and the lysate was stored.

##### QUANTITATIVE DETECTION OF HUMAN P53

The wells coated with monoclonal antibody on the microwell strips were activated with 300  $\mu\text{L}$  of wash buffer. Standard of p53 ranging from 50 U/mL to 0.8 U/mL was used in this assay. Sample diluent was used as blank. Subsequently, 50  $\mu\text{L}$  of Biotin-Conjugate was placed into the wells including the blank wells and incubated. Then, the plate was cleared and 100  $\mu\text{L}$  of Streptavidin-HRP was added and incubated for 1 h at room temperature. The wells were rinsed and 100  $\mu\text{L}$  of TMB substrate was added and kept at room temperature (18 - 25 °C) for 10 min in the dark. The reaction was ceased using stop solution and the plate was read instantly using a microplate ELISA (Sunrise, Tecan, Austria) reader at 450 nm.

#### BCL-2 AND BAX EXPRESSION

ELISA FOR QUANTITATIVE DETECTION OF HUMAN BCL-2 Human Bcl-2 ELISA Kit from Bendermed Systems (Austria) was used to perform the assay. The standard Bcl-2 ranged from 32 to 0.5 ng/mL. One hundred

microlitre of sample diluent was used as blank. After the incubation period 72 h, cell lysate was obtained following the addition of Cell Lysis Buffer and 1 h of incubation at room temperature. Twenty microlitre of cell lysate and 80  $\mu$ L of sample diluent were pipetted into the sample wells. Subsequently, 50  $\mu$ L of Biotin-Conjugate was added. The samples were kept for 2 h at room temperature (18 - 25 °C) at 100 rpm. The plate was washed, 100  $\mu$ L of diluted Streptavidin-HRP was added and incubated for 1 h at room temperature. The supernatant was discarded and washed. One hundred microlitre of TMB substrate was pipetted and kept at room temperature (18 - 25 °C) for 10 min in the dark. Then, the reaction was ceased by adding 100  $\mu$ L of stop solution and the plate was read quickly with a microplate ELISA reader (Sunrise, Tecan, Austria) at 450 nm.

#### HUMAN BAX ENZYME IMMUNOMETRIC ASSAY

The Human Bax Enzyme Immunometric Assay from Assay Design was used to carry out this assay. The samples collected after 72 h of incubation were resuspended in modified Cell Lysis Buffer to prepare the cell lysates. One hundred microlitre of Assay Buffer was added into a well as a blank. One hundred microliter of Bax standard was added into appropriate wells. Then, 100  $\mu$ L of cell lysate was pipetted into the wells and kept for 1 h at room temperature while rotating at 500 rpm. Then, the wells were rinsed off and 100  $\mu$ L of yellow antibody was pipetted into each well. Following an hour of incubation, the plate was washed and of 100  $\mu$ L of blue conjugate was pipetted into the well. The plate was kept for 30 min at room temperature at 500 rpm. Then, the plate was washed, 100  $\mu$ L of substrate solution was added and kept for another 30 min. The reaction was ended by adding 100  $\mu$ L of stop solution and read instantly at 450 nm using microplate ELISA reader (Sunrise, Tecan, Austria).

#### STATISTICAL ANALYSIS

The data are displayed as mean  $\pm$  SEM. Student's t-test and One-way ANOVA were used for multiple comparisons. The level of significance was set as  $p < 0.05$ .

### RESULTS

#### DAMNACANTHAL'S CYTOTOXICITY TOWARDS CEM-SS CELL LINE

Figure 1 depicts that at 24 h of incubation period, there were no differences ( $p > 0.05$ ) on the percentage of

viability between the control and treated cells in every concentration (1, 3, 10, and 30  $\mu$ g/mL). After 48 and 72 h of incubation, the cell viability of the treated sample (30  $\mu$ g/mL) reduced significantly ( $p < 0.05$ ) from 100% to 49.26%, and 40.4%, respectively. The most prominent reduction of cell viability following treatment with 30  $\mu$ g/mL of damnacanthal.

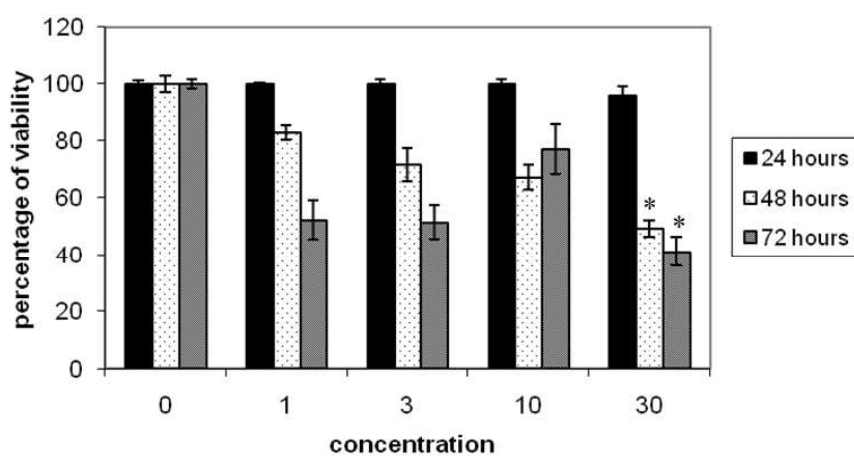
#### MORPHOLOGICAL ANALYSIS

At 24 h, there were no differences in cell density and cell features of the treated samples at all concentrations of damnacanthal (1, 3, 10, and 30  $\mu$ g/mL) as compared to the control (Figure 2). Untreated cells showed regular round shape with similarity in size. The cells are shiny and intact. Prominent changes can be observed in the treated cells especially at the 10 and 30  $\mu$ g/mL concentrations of damnacanthal after 48 and 72 h incubation with a lot of the remnants of dead cells or cell debris. Lower density of cells was observed at higher concentration of damnacanthal (10 and 30  $\mu$ g/mL) following 48 and 72 h of incubation. As compared to untreated cell (Figure 3(A)), cells treated with damnacanthal indicated some key apoptotic features such as denser and more concentrated cytoplasm, membrane-bounded apoptotic body which was separated from the mother cell, compaction of nucleus, blebbing of the cell and secondary necrosis especially in the sample at 30  $\mu$ g/mL of damnacanthal treatment (Figure 3(B) and 3(C)).

#### CELL CYCLE ANALYSIS

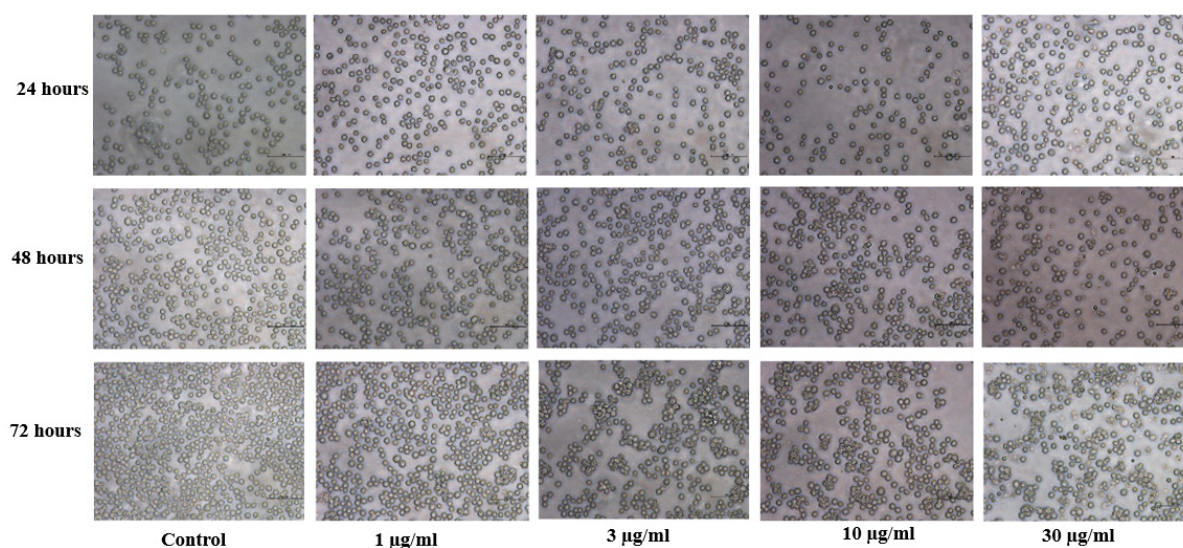
Flow cytometry analysis of PI-stained cells showed a typical diploid DNA peak in cells untreated with damnacanthal (control). No changes in the pattern of the cell accumulation in treated (1, 3, 10, and 30  $\mu$ g/mL) was observed as compared to the untreated samples after 24 and 48 h of incubation (Figure 4). However, after 72 h of incubation, there was a substantial difference ( $p < 0.05$ ) in G0/G1 cell percentage in the sample treated with 30  $\mu$ g/mL of damnacanthal (44.61%) compared to the control (62.08%) (Figure 4).

The higher the concentration of damnacanthal, the higher number of cells in the G2/M phase were detected. The population increased significantly ( $p < 0.05$ ) to 23.16% at 30  $\mu$ g/mL of damnacanthal treatment whereby the control cells recorded only 7.50%. Thus, damnacanthal arrested the cell at G2/M phase. However, after 72 h of incubation, proliferation of damnacanthal treated cells increased while untreated cells decreased. The readings on the cell population at every phase for 24, 48, and 72 h of treatment were further summarized in Table 1.



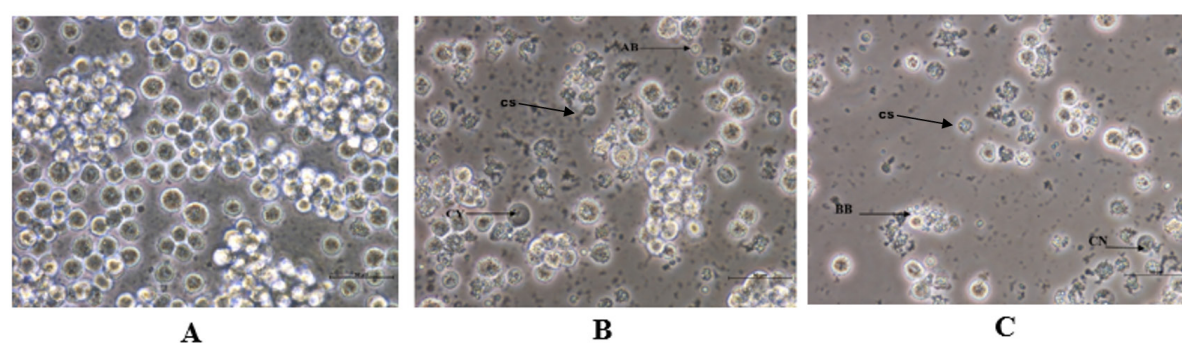
Data presented as mean  $\pm$  standard error. \* indicate significant difference at  $p < 0.05$  compared to control. Each experiment was performed in triplicate

FIGURE 1. Damnacanthal (0, 1, 3, 10 and 30  $\mu\text{g/mL}$ ) treated CEM-SS cells viability after 24, 48 and 72 h



Images are captured at 400X magnification

FIGURE 2. Microscopic images of damnacanthal (0, 1, 3, 10 and 30  $\mu\text{g/mL}$ ) treated CEM-SS cells after 24, 48 and 72 h



Images are captured at 400X magnification. The arrows indicate distinguished characteristics of apoptosis; condensation of cytoplasm (CY), membrane-bounded apoptotic body (AB), compaction of nucleus (CN), cell shrinkage (CS) and the blebbing of the cell (BB)

FIGURE 3. CEM-SS cells (A) Untreated (B and C) after 72 h incubation with 30  $\mu\text{g/mL}$  damnacanthal

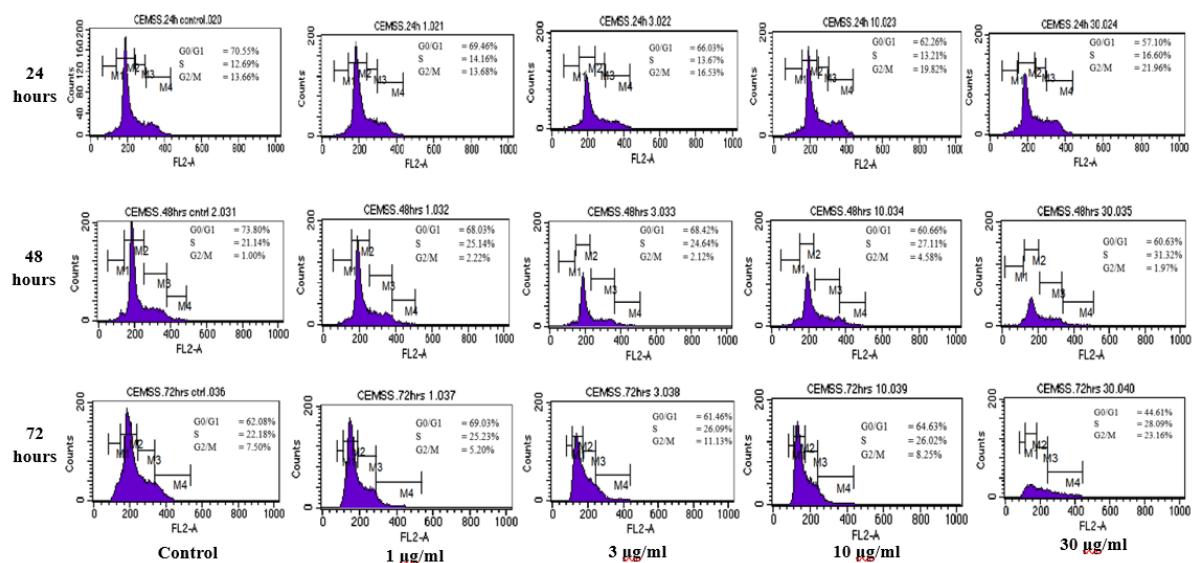


FIGURE 4. Dose- and time-dependent PI stained-flow cytometry cell cycle analysis of damnacanthal (0, 1, 3, 10 and 30 µg/mL) treated CEM-SS cells after 24, 48 and 72 h

#### DETERMINATION OF DAMNACANTHAL EFFECTS TOWARDS P53 MUTANT

Table 2 summarizes damnacanthal's effects towards p53 mutant. Higher readings of optical density indicate higher level of p53. The readings were found to exceed the range of standard curve, even at very high serial dilution (1:8). According to the manufacturer, readings exceeding OD of 2.0 represent very high level of p53. Nevertheless, it has been shown that the level of p53 did not vary ( $p > 0.05$ ) in cells treated with all concentrations of damnacanthal (1, 3, 10, and 30 µg/mL) compared to control.

#### CASPASE 2 AND 6 ACTIVATION

After 24 hours of treatment incubation, all treatments with damnacanthal (1, 3, 10, and 30 µg/mL) showed no changes ( $p > 0.05$ ) in the level of caspase 2, 3, 6, 8 and 9 as compared to the untreated cells (Figure 5(A)). Following a 72 h incubation with the treatment, the level of caspase 2 and 6 increased ( $p < 0.05$ ) compared to the control and caspases 3, 8 and 9 (Figure 5(B)).

#### ANALYSIS ON LEVEL OF BCL-2/BAX

Level of Bcl-2 and Bax activity decreased and increased insignificantly ( $p < 0.05$ ), respectively, in cells treated with 30 µg/mL of damnacanthal compared to the control group after 72 h incubation (Figure 6).

#### DISCUSSION

Agents that are cytotoxic to cancer cells are of interest to be developed as chemotherapy drugs. Mostly, chemotherapy agents alter the functions and changes the RNA, DNA or protein synthesis in the cells leading to cell death. In this study, damnacanthal was found to cause the reduction on cell viability and morphological changes at a higher dose following a longer incubation period. Damnacanthal at 10 and 30 µg/mL reduced cell viability indicating its cytotoxic effects towards CEM-SS cell line. The cytotoxicity activities of damnacanthal at the exact doses used in this study have been published in Latifah et al (2021). We have carried out MTT assay on non-tumour cell lines to confirm the toxicity of damnacanthal (data not included in this manuscript). Damnacanthal showed no toxicity ( $IC_{50} > 30$  µg/mL) in human peripheral blood mononuclear (PBMC), mouse embryo (3T3) and monkey kidney fibroblast (Vero). Therefore, the highest dose of damnacanthal treatment was set to be at 30 µg/mL.

Cells treated with damnacanthal showed no morphological alterations as compared to the untreated cells after 24 h of incubation. However, after the incubation for 48 and 72 h, the treated cells exhibited typical characteristics features of programmed cell death such as convolution of nuclear and cellular outline, chromatin and cytoplasm condensation, disintegration of nucleus and blebbing formation of plasma membrane

(Povea-Cabello et al. 2017). Cells in the 30  $\mu\text{g}/\text{mL}$  of damnacanthal treatment at 48 h, showed cell shrinkage. The change in the cell morphology happens as a result of a net outward flow of the cell fluid, probably due to the blockage of the  $\text{Na}^+ - \text{K}^+ - \text{Cl}^-$  cotransporter system (Allen, Hunter III & Agrawal 1997). At this time, dense chromosome occurs at the periphery of nucleus which leads to the formation of compacted and segregated chromatin (Johnson 2006).

As the chromatin in the nucleus becomes condensed, both the nuclear membrane and plasma membrane contract, causing the cell to have a bubbling surface or appearing blebbed (Allen, Hunter III & Agrawal 1997). Keratin breakdown will eventually be causing the cell to undergo cytoplasmic and nuclear reorganization, resulting in the disassembly of the nuclear and cytoskeletal components during cell death (Schutte et al. 2004). During blebbing, apoptotic bodies are formed when chromatins undergo condensation and segregation when the nucleus disassembles forming nuclear fragments present inside a two-layered nuclear envelope (Allen, Hunter III & Agrawal 1997). The entire nucleus fragments due to endonucleases such as apoptosis-inducing factors and caspase-activated DNase. The endonucleases cut the longwinded of DNA into shorter strands containing about 200 bp representing apoptosis (Basnakian & Moore 2021).

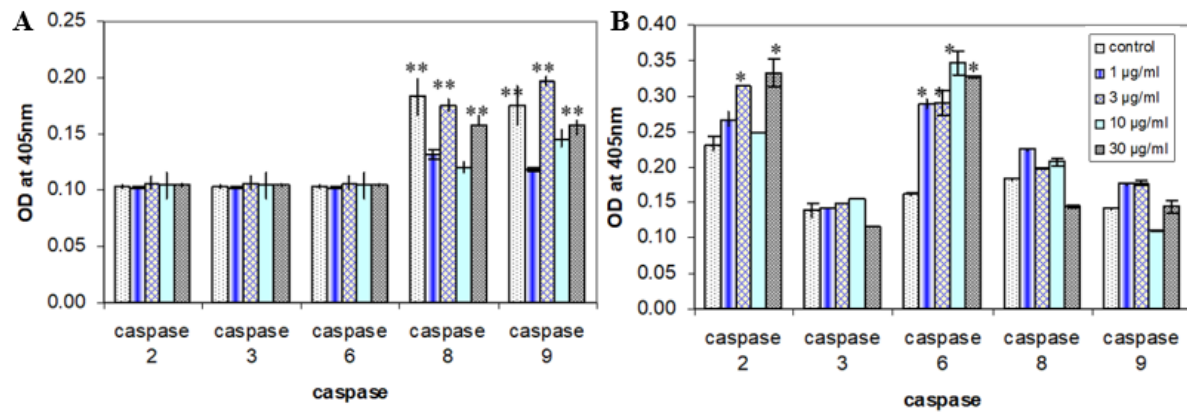
In this study, there was no sub-G1 peak detected, indicating the presence of apoptosis. Damnacanthal leads to cell cycle cessation at the G2/M phase. Similar finding was reported when damnacanthal by increasing p27Kip1 protein with reducing cyclin D1 protein levels in SKVO3 ovarian cancer cells (Li et al. 2022), increases the population of cells in the S phase of H400 oral cancer cells (Shaghayegh et al. 2017) and G1 phase of MCF-7 breast (Aziz et al. 2014). These outcomes apparently put forward a possibility that damnacanthal induced both cell cycle arrest and apoptosis towards CEM-SS cells.

No apparent difference ( $p > 0.05$ ) was observed in the p53 levels between cells treated and untreated with damnacanthal. It is well-known that p53 regulates a G2 checkpoint through cyclin B1 and is crucial for the cell's apoptotic activity (Shieh et al. 2004). p53 was found to inhibit cells transition from G2/M phase into the second-round replication phase by increasing the transcription of 14-3-3 $\sigma$  which later combines with cdc25c phosphatase and hinders the access of cdc25c into the nucleus. This prevents the DNA from further replication eventually causing cell cycle arrest (Foster 2008). However, judging the outcome of this study, it is projected that damnacanthal caused the cell cycle arrest

through p53 independent pathway. The p53 level was found to be overexpressed in both treated and untreated cells. With the findings, we suggest that damnacanthal induced apoptosis through p53-independent pathway.

This study presented no changes ( $p > 0.05$ ) in the level of caspase 2, 3, 6, 8, and 9 after 24 h of treatment with damnacanthal possibly due to absence of apoptosis in line with our flow cytometry study. Even though at 48 h after incubation with damnacanthal prominent changes indicating apoptotic activities, only a fraction of the cells was undergoing apoptosis. Whereas, at the final sampling point of 72 post incubation, majority of the CEM-SS cells were undergoing apoptosis. Therefore, the caspase level was only measured at the initial (24 h) and final (72 h) time point of the treatment. Caspases activation is required for apoptosis (Parrish, Freel & Kornbluth 2013; Van Opdenbosch & Lamkanfi 2019). Even though caspase 3, 8, and 9 are the crucial players in inducing apoptosis (Prasad et al. 2006), their level of activities in damnacanthal-treated cells was similar ( $p > 0.05$ ) to the control. Instead, the levels of caspase 2 and 6 was elevated ( $p < 0.05$ ) in cells treated with damnacanthal at 30  $\mu\text{g}/\text{mL}$  after 72 h of incubation. Damnacanthal arrested the cell at G2/M phase and eventually induced apoptosis in the cells through the activation of caspase 2 and caspase 6 in a dose- and time-dependent manner. Caspase 6 targets Lamin A protein that affect the integrity of nuclear membrane (Hubner et al. 2006). Caspase 6 is also responsible in cleaving Keratin 18 which causes cytoskeletal collapse (Stennick & Salvesen 1998). Keratin breakdown leads the cell to undergo cytoplasmic and nuclear reorganization which is accompanied by processes such as condensation, and later resulting in the disassembly of the nuclear and cytoskeletal components during cell death (Schutte et al. 2004). Klaiman, Champagne and LeBlanc (2009) stated that caspase 6 was found to be self-processed and self-activated unlike other caspases.

Caspase 2 is unique since it plays a role as initiator and effector caspase (Zhivotovsky & Orrenius 2005). Caspase-2 is required for an apoptotic response to neurotrophic deprivation and DNA damage, a subset of intrinsic stimuli (Boatright & Salvesen 2003). Caspase 2 acts on mitochondria, to mediate the apoptotic process and to activate caspase 8. Caspase 8 in turn plays a role in executioner caspase 3 activation (Huang et al. 2007). Yet, this study showed no involvement of both caspase 8 and caspase 3. This is most probably due to caspase 2's role in the mitochondrial apoptotic pathway, which needs zymogen but not the associated proteolytic activity (Zhivotovsky & Orrenius 2005).



Data presented as mean  $\pm$  standard error. \*indicates significant difference at  $p < 0.05$  compared to control. Each experiment was performed in triplicate

FIGURE 5. Caspase levels in damnacanthal (0, 1, 3, 10, and 30  $\mu\text{g}/\text{mL}$ ) treated CEM-SS cells after (A) 24 and (B) 72 h of incubation. The experiment was carried out according to vendor's protocol with 1:6 of working dilution. The caspase level is expressed by the optical density value (OD) at 405 nm

TABLE 1. Flow cytometry cell cycle analysis of damnacanthal (0, 1, 3, 10 and 30  $\mu\text{g}/\text{mL}$ ) treated CEM-SS cells after 24, 48 and 72 h

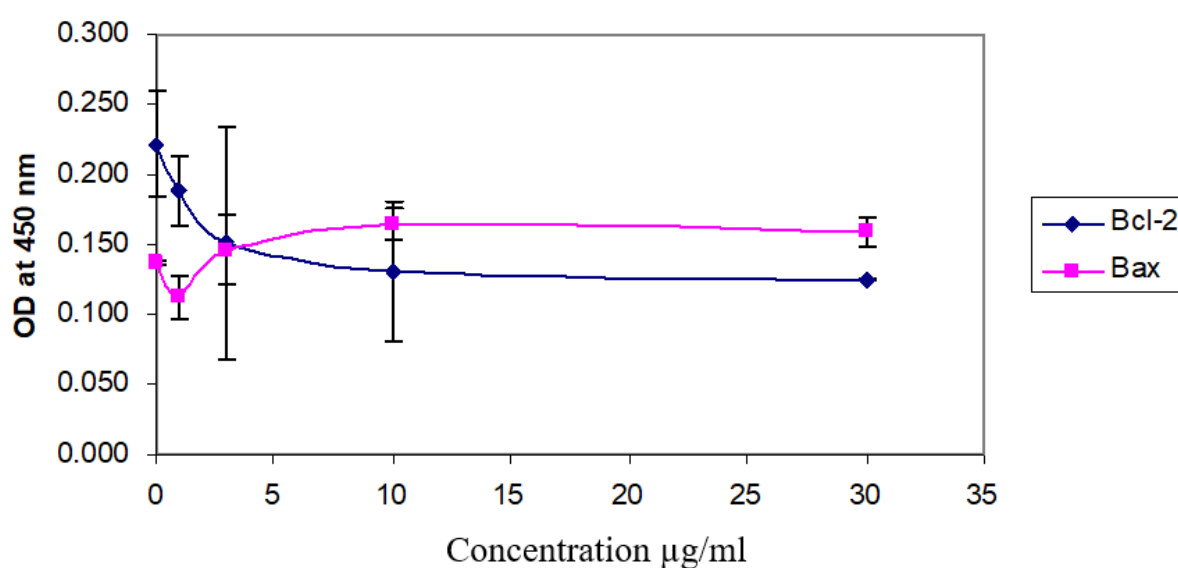
Cell cycle phase	Concentration $\mu\text{g}/\text{mL}$				
	0	1	3	10	30
<b>24 hours</b>					
Sub-G1 (M1)	2.91 $\pm$ 0.04	2.37 $\pm$ 0.17	2.96 $\pm$ 0.11	3.24 $\pm$ 0.12	3.54 $\pm$ 0.05
G0/G1 (M2)	70.12 $\pm$ 0.52	69.28 $\pm$ 0.24	66.41 $\pm$ 0.51	63.82 $\pm$ 0.22	59.12 $\pm$ 1.01
S (M3)	12.27 $\pm$ 0.23	13.54 $\pm$ 0.32	13.71 $\pm$ 0.09	14.07 $\pm$ 0.5	16.08 $\pm$ 0.26
G2/M (M4)	14.61 $\pm$ 0.59	14.71 $\pm$ 0.51	16.7 $\pm$ 0.33	18.7 $\pm$ 0.57	20.99 $\pm$ 0.48
<b>48 hours</b>					
Sub-G1 (M1)	3.53 $\pm$ 0.1	4.46 $\pm$ 0.34	3.83 $\pm$ 0.57	7.36 $\pm$ 0.81	6.92 $\pm$ 4.25
G0/G1 (M2)	74.12 $\pm$ 0.17	69.85 $\pm$ 2.71	70.17 $\pm$ 2.61	65.93 $\pm$ 5.04	56.92 $\pm$ 3.69
S (M3)	20.38 $\pm$ 0.52	21.99 $\pm$ 2.37	21.45 $\pm$ 2.56	23.64 $\pm$ 3.21	29.07 $\pm$ 1.63
G2/M (M4)	1.95 $\pm$ 0.19	2.19 $\pm$ 0.1	2.05 $\pm$ 0.04	3.36 $\pm$ 0.64	3.47 $\pm$ 1.72
<b>72 hours</b>					
Sub-G1 (M1)	6.22 $\pm$ 1.20	1.91 $\pm$ 0.71	2.35 $\pm$ 0.34	2.17 $\pm$ 0.32	4.23 $\pm$ 0.21
G0/G1 (M2)	63.22 $\pm$ 0.58	66.71 $\pm$ 2.01	62.91 $\pm$ 1.4	62.78 $\pm$ 0.96	46.9 $\pm$ 1.26
S (M3)	22.98 $\pm$ 0.48	26.2 $\pm$ 0.97	25.79 $\pm$ 0.46	26.08 $\pm$ 0.03	27.25 $\pm$ 0.74
G2/M (M4)	6.75 $\pm$ 0.38	5.54 $\pm$ 0.25	10.4 $\pm$ 0.64	9.11 $\pm$ 0.5	21.77 $\pm$ 0.7



TABLE 2. p53 levels in damnacanthal (0, 1, 3, 10 and 30  $\mu\text{g/mL}$ ) treated CEM-SS cells after 24, 48 and 72 h. The p53 level is expressed by the optical density value (OD) at 450 nm

Concentration $\mu\text{g/mL}$	OD at 450 nm		
	24	48	72
0	$3.51 \pm 0.05$	$3.71 \pm 0.01$	$3.60 \pm 0.08$
1	$3.57 \pm 0.08$	$3.74 \pm 0.01$	$3.58 \pm 0.17$
3	$3.62 \pm 0.02$	$3.76 \pm 0.01$	$3.60 \pm 0.05$
10	$3.64 \pm 0.05$	$3.73 \pm 0.02$	$3.80 \pm 0.04$
30	$3.62 \pm 0.02$	$3.87 \pm 0.02$	$3.85 \pm 0.05$

Data is presented as mean  $\pm$  SEM. \*  $p < 0.05$  treatment vs control. Each experiment was performed in triplicate



Data presented as mean  $\pm$  standard error \*indicates significant difference at  $p < 0.05$  compared to control. Each experiment was performed in triplicate

FIGURE 6. Bcl-2 and Bax activity levels after 72 h incubation. The Bcl-2 and Bax level are expressed by the optical density value (OD) at 450 nm

Quinones are known as highly redox active molecule. It uses the semiquinone radicals to redox cycle and forms the reactive oxygen species (ROS) (Su et al. 2005). This characteristic is also exhibited by damnacanthal, an anthraquinone, a part of quinone which is a very cytotoxic compound towards CEM-SS cells (Ali et al. 2000) and possesses high efficiencies in generating ROS (Abu et al. 2014; Rajendran et al. 2004). The ROS generation leads to DNA strand scission primarily at guanines which a possible mechanism of the formation of DNA fragmentation ladder that is known as a sign of apoptosis (Fukuhara et al. 2007). Previous study by Latifah et al. (2021) showed that CEM-SS cell treated with damnacanthal induced apoptosis by formation of DNA fragmentation ladder. The generation of ROS is responsible for the cell to

undergo caspase 2 dependent apoptosis (Prasad et al. 2006). ROS is also known to activate p21 which leads to p53-independent apoptosis (Schonthal, Mueller & Cadenas 2000). This study's outcome suggested that the cells underwent apoptosis through intrinsic pathway via caspase 2 activation due to the induction of ROS generation by damnacanthal. Thus, caspase 2 may act independently by engaging directly towards the mitochondria due to the activation of ROS (Prasad et al. 2006; Zhivotovsky & Orrenius 2005) whereas caspase 6 which is able to self-activate (Klaiman, Champagne & LeBlanc 2009) acts directly towards the Lamin A protein (Schutte et al. 2004) triggering apoptosis.

Apoptosis depends on the activation of Bcl-2 and Bax (Chen et al. 2004). Thus, in this study, to elucidate the involvement of the proteins in CEM-SS cells treated

with damnacanthal, 72 h was chosen as majority of them showed characteristics of apoptosis. Reduced activity of Bcl-2 and increased activity of Bax was observed in cells in the 30 µg/mL of damnacanthal treatment group. According to Heiser et al. (2004), Bcl-2 is an antiapoptotic protein while Bax supports apoptosis. The relative concentrations of both these proteins would determine either survival or death of the cell (Park et al. 2008).

The nuclear membrane, mitochondria and endoplasmic reticulum are the prime sites where Bcl-2 is contained. These aforementioned sites are also where the formation oxygen-free radical mostly occurs and their apoptotic effect is exerted (Su et al. 2005). According to Su et al. (2005), Bcl-2 might deter apoptosis by scavenging oxygen derived free radicals present within the cell. However, phosphorylated Bcl-2 can cause inactivation of its anti-apoptotic function (Tamura, Simizu & Osada 2004). According to Tseng et al. (2002), Bcl-2 phosphorylation plays a role in G2/M cell cycle arrest and apoptosis which is consistent with the result of cell cycle arrest in this study. Furthermore, damnacanthal was found to possess high photogeneration efficiencies in generating ROS (Rajendran et al. 2004). Thus, it may be presumed that with inability of Bcl-2 to carry out its anti-apoptotic role, the formation of ROS may lead to mitochondrial damage resulting in cell death (Su et al. 2005). Bax could homodimerize and form heterodimers with Bcl-2. An overexpression of Bax could lessen Bcl-2's death repressor activity (Cheng et al. 2007).

When an apoptotic stimulus is present, Bax, which is typically present as a cytosolic monomer undergoes structural alterations and integrates with the outer mitochondrial membrane triggering the development of supramolecular pores which mediates permeabilization of mitochondria membrane (Buytaert, Dewaele & Agostinis 2007; Hussar 2022). This enables cytochrome c to pass through this channel (Lee et al. 2001). Cytochrome c released into the cytosol from mitochondria induces apoptosome formation which then causes caspases to be activated (Brown & Borutaite 2008). Caspases involved in the process are referred to as initiator caspases such as caspase 8 and caspase, that either directly or indirectly effector caspases such as caspase 3, 6, and 7 (Lee et al. 2001). Thus, caspase 8 and 9 have been widely accepted as the most important players in caspase cascade in inducing apoptosis (Prasad et al. 2006). In this study however, low activity of these caspases was observed. Instead, caspase 2 and caspase 6 showed high activity. From previous work on emodin, Su et al. (2005) suggested caspase 2 activation is also dependent on cytochrome c release to cytosol. On the other hand, caspase 6 was said to be self-processed

and self-activated unlike other caspases (Klaiman, Champagne & LeBlanc 2009). Therefore, this result may suggest that cytochrome c release may trigger the initiation of caspase 2 directly and caspase 6 indirectly. The result of this study suggests that damnacanthal induces apoptosis of the CEM-SS cells by elevating the level of Bax and lowering the level of Bcl-2 activities. Further study is required to identify other mechanisms such as Bcl-2 phosphorylation which might be involved in this subject.

Moving forward, there are two crucial mediators, cyclin B1/CDK1 and p21 that should be studied. The genomes integrity is protected and maintained by the cell cycle checkpoints, at the presence of many stress signals. If the checkpoints are compromised, cancer could develop and any form of anticancer treatments are negatively influenced. This cell cycle mechanism is highly impacted by cyclin B1/CDK1 and p21. p21, either via p53-dependant or independent pathways, promotes tumorigenesis principally by inhibiting the progression of the cell cycle and allowing DNA repair. On the other hand, cyclin B1/CDK1 is involved in the expression of p53 regulation at G2 checkpoint (Al Bitar & Gali-Muhtasib 2019). Therefore, further understanding on the apoptotic mechanism could be attained if the expression of these two mediators is evaluated.

#### CONCLUSION

Damnacanthal reduced the cell viability and caused morphological changes to the human CEM-SS cell line at a higher dose (10 and 30 µg/mL) following a longer incubation period of 72 h indicating its cytotoxic effects. No sub-G1 peak was detected in the flow cytometry analyses confirming the occurrence of apoptosis. Damnacanthal arrested the cell at G2/M phase and eventually induced apoptosis in the cells through the caspase 2 and 6's activation at the highest concentration of damnacanthal (30 µg/mL) after 72 h of treatment. No activation of caspases 3, 8, and 9 were detected. No alteration to the p53 levels following treatment with damnacanthal indicated to apoptosis induction via p53-independent pathway. Reduced activity of Bcl-2 and increased activity of Bax, the anti- and pro-apoptotic proteins, respectively was observed in cells treated with damnacanthal at 30 µg/mL determines the survival of the cells.

#### REFERENCES

- Abu, N., Ali, N.M., Ho, W.Y., Yeap, S.K., Aziz, M.Y. & Alitheen, N.B. 2014. Damnacanthal: A promising compound as a medicinal anthraquinone. *Anti-Cancer Agents in Medicinal Chemistry* 14(5): 750-755. doi: 10.2174/18715206113136660366

- Al Bitar, S. & Gali-Muhtasib, H. 2019. The role of the cyclin dependent kinase inhibitor p21<sup>cip1/waf1</sup> in targeting cancer: Molecular mechanisms and novel therapeutics. *Cancers (Basel)* 11(10): 1475. doi: 10.3390/cancers11101475
- Ali, A., Ismail, N., Mackeen, M., Yazan, L., Mohamed, S., Ho, A. & Lajis, N. 2000. Antiviral, cytotoxic and antimicrobial activities of anthraquinones isolated from the roots of *Morinda elliptica*. *Pharmaceutical Biology* 38: 298-301. doi: 10.1076/1388-0209(200009)3841-AFT298
- Allen, R.T., Hunter III, W.J. & Agrawal, D.K. 1997. Morphological and biochemical characterization and analysis of apoptosis. *Journal of Pharmacological and Toxicological Methods* 37(4): 215-228. doi: 10.1016/s1056-8719(97)00033-6
- Anand, U., Dey, A., Chandel, A.K.S., Sanyal, R., Mishra, A., Pandey, D.K., De Falco, V., Upadhyay, A., Kandimalla, R., Chaudhary, A., Dhanjal, J.K., Dewanjee, S., Vallamkondu, J. & Pérez de la Lastra, J.M. 2022. Cancer chemotherapy and beyond: Current status, drug candidates, associated risks and progress in targeted therapeutics. *Genes & Diseases* 10(4): 1367-1401. doi: 10.1016/j.gendis.2022.02.007
- Aziz, M.Y., Omar, A.R., Subramani, T., Yeap, S.K., Ho, W.Y., Ismail, N.H., Ahmad, S. & Alitheen, N.B. 2014. Damnacanthal is a potent inducer of apoptosis with anticancer activity by stimulating p53 and p21 genes in MCF-7 breast cancer cells. *Oncology Letters* 7(5): 1479-1484. doi: 10.3892/ol.2014.1898
- Basnakian, A.G. & Moore, C.L. 2021. Apoptotic DNase network: Mutual induction and cooperation among apoptotic endonucleases. *Journal of Cellular and Molecular Medicine* 25(14): 6496-6499. doi: 10.1111/jcmm.16665
- Boatright, K.M. & Salvesen, G.S. 2003. Mechanisms of caspase activation. *Current Opinion in Cell Biology* 15: 725-731. doi: 10.1016/j.ceb.2003.10.009
- Brown, G.C. & Borutaite, V. 2008. Regulation of apoptosis by the redox state of cytochrome c. *Biochimica et Biophysica Acta* 1777: 877-881. doi: 10.1016/j.bbabi.2008.03.024
- Buytaert, E., Dewaele, M. & Agostinis, P. 2007. Molecular effectors of multiple cell death pathways initiated by photodynamic therapy. *Biochimica et Biophysica Acta* 1776: 86-107. doi: 10.1016/j.bbcan.2007.07.001
- Chen, H.C., Hsieh, W.T., Chang, W.C. & Chung, J.G. 2004. Aloe-emodin induced *in vitro* G2/M arrest of cell cycle in human promyelocytic leukemia HL-60 cells. *Food and Chemical Toxicology* 42: 1251-1257. doi: 10.1016/j.fct.2004.03.002
- Cheng, A.C., Jian, C.B., Huang, Y.T., Lai, C.S., Hsu, P.C. & Pan, M.H. 2007. Induction of apoptosis by *Uncaria tomentosa* through reactive oxygen species production, cytochrome c release, and caspases activation in human leukemia cells. *Food and Chemical Toxicology* 45: 2206-2218. doi: 10.1016/j.fct.2007.05.016
- Chipuk, J.E., Kuwana, T., Bouchier-Hayes, L., Droin, N.M., Newmeyer, D.D., Schuler, M. & Green, D.R. 2004. Direct activation of Bax by p53 mediates mitochondrial membrane permeabilization and apoptosis. *Science* 303(5660): 1010-1014. doi: 10.1126/science.1092734
- Chong, T.M., Abdullah, M.A., Fadzillah, N.M., Lai, O.M. & Lajis, N.H. 2005. Jasmonic acid elicitation of anthraquinones with some associated enzymic and non-enzymic antioxidant responses in *Morinda elliptica*. *Enzyme and Microbial Technology* 36: 469-477. <https://doi.org/10.1016/j.enzmictec.2004.11.002>
- Dvory-Sobol, H., Cohen-Noyman, E., Kazanov, D., Figer, A., Birkenfeld, S., Madar-Shapiro, L., Benamouzig, R. & Arber, N. 2006. Celecoxib leads to G2/M arrest by induction of p21 and down-regulation of cyclin B1 expression in a p53-independent manner. *European Journal of Cancer* 42: 422-426. doi: 10.1016/j.ejca.2005.11.009
- Foster, I. 2008. Cancer: A cell cycle defect. *Radiography* 14: 144-149. <https://doi.org/10.1016/j.radi.2006.12.001>
- Fukuhara, K., Oikawa, S., Hakoda, N., Sakai, Y., Hiraku, Y., Shoda, T., Saito, S., Miyata, N., Kawanishi, S. & Okuda, H. 2007. 9-Nitroanthracene derivative as a precursor of anthraquinone for photodynamic therapy. *Bioorganic and Medicinal Chemistry* 15: 3869-3873. doi: 10.1016/j.bmc.2007.03.029
- García-Vilas, J.A., Quesadal, A.R. & Medina, M.A. 2015. Damnacanthal, a noni anthraquinone, inhibits c-Met and is a potent antitumor compound against Hep G2 human hepatocellular carcinoma cells. *Scientific Reports* 5: 8021. doi: 10.1038/srep08021
- GLOBOCAN. 2020. <https://gco.iarc.fr/today/data/factsheets/populations/458-malaysia-fact-sheets.pdf> (Accessed 3 May 2023).
- Green, D.R. 2022. Caspases and their substrates. *Cold Spring Harbor Perspectives in Biology* 14: a041012. doi: 10.1101/cshperspect.a041012
- Heiser, D., Labi, V., Erlacher, M. & Villunger, A. 2004. The Bcl-2 protein family and its role in the development of neoplastic disease. *Experimental Gerontology* 39: 1125-1135. doi: 10.1016/j.exger.2004.04.011
- Hirazumi, A., Furusawa, E., Chou, S.C. & Hokama, Y. 1996. Immunomodulation contributes to the anticancer activity of *Morinda citrifolia* (Noni) fruit juice. *Proceedings of the Western Pharmacology Society* 39: 7-9.
- Hounsell, C. & Fan, Y. 2021. The duality of caspases in cancer, as told through the fly. *International Journal of Molecular Sciences* 22(16): 8927. doi: 10.3390/ijms22168927
- Huang, P., Akagawa, K., Yokoyama, Y., Nohara, K., Kano, K. & Morimoto, K. 2007. T-2 toxin initially activates caspase-2 and induces apoptosis in U937 cells. *Toxicology Letters* 170(1): 1-10. doi: 10.1016/j.toxlet.2006.05.017

- Hubner, S., Eam, J.E., Hubner, A. & Jans, D.A. 2006. Laminopathy-inducing lamin A mutants can induce redistribution of lamin binding proteins into nuclear aggregates. *Experimental Cell Research* 312: 171-183. doi: 10.1016/j.yexcr.2005.10.011
- Hussar, P. 2022. Apoptosis regulators Bcl-2 and caspase-3. *Encyclopedia* 2(4): 1624-1636. <https://doi.org/10.3390/encyclopedia2040111>
- Ismail, N., Mohamad, H., Mohidin, A. & Lajis, N.H. 2002. Antioxidant activity of anthraquinones from *Morinda elliptica*. *Natural Product Sciences* 8: 48-51. [https://www.researchgate.net/publication/289830185\\_Antioxidant\\_activity\\_of\\_anthraquinones\\_from\\_Morinda\\_elliptica](https://www.researchgate.net/publication/289830185_Antioxidant_activity_of_anthraquinones_from_Morinda_elliptica)
- Johnson, L.R. 2006. Apoptosis in the Gastrointestinal Tract. In *Physiology of the Gastrointestinal Tract*. 4th ed., edited by Johnson, L.R., Barret, E.K., Ghishan, F.K., Merchant, J.L., Said, H.M. & Wood, J.D. Massachusetts: Academic Press. pp. 345-373.
- Katta, B., Vijayakumar, C., Dutta, S., Dubashi, B. & Nelamangala Ramakrishnaiah, V.P. 2023. The incidence and severity of patient-reported side effects of chemotherapy in routine clinical care: A prospective observational study. *Cureus* 15(4): e38301. doi: 10.7759/cureus.38301
- Klaiman, G., Champagne, N. & LeBlanc, A.C. 2009. Self-activation of caspase-6 *in vitro* and *in vivo*: Caspase-6 activation does not induce cell death in HEK293T cells. *Biochimica et Biophysica Acta* 1793: 592-601. doi: 10.1016/j.bbamcr.2008.12.004
- Klucar, J. & al-Rubeai, M. 1997. G2 cell cycle and apoptosis are induced in Burkitt's lymphoma cells by anticancer agent oracin. *FEBS Letters* 400(1): 127-130. doi: 10.1016/S0014-5793(96)01307-5
- Latifah, S.Y., Gopalsamy, B., Abdul Rahim, R., Manaf Ali, A. & Haji Lajis, N. 2022. Ultrastructural and morphological effects in T-lymphoblastic leukemia CEM-SS cells following treatment with nordamnacanthal and damnacanthal from roots of *Morinda elliptica*. *Molecules* 27(13): 4136. doi: 10.3390/molecules27134136
- Latifah, S.Y., Gopalsamy, B., Abdul Rahim, R., Manaf Ali, A. & Haji Lajis, N. 2021. Anticancer potential of damnacanthal and nordamnacanthal from *Morinda elliptica* roots on T-lymphoblastic leukemia cells. *Molecules* 26(6): 1554. doi: 10.3390/molecules26061554
- Lee, H.Z., Hsu, S.L., Liu, M.C. & Wu, C.H. 2001. Effects and mechanisms of aloe-emodin on cell death in human lung squamous cell carcinoma. *European Journal of Pharmacology* 431: 287-295. doi: 10.1016/S0014-2999(01)01467-4
- Li, R., Li, H., Lan, J., Yang, D., Lin, X., Xu, H., Han, B., Yang, M., Su, B., Liu, F. & Jiang, W. 2022. Damnacanthal isolated from *Morinda* species inhibited ovarian cancer cell proliferation and migration through activating autophagy. *Phytomedicine* 100(2022): 154084. doi: 10.1016/j.phymed.2022.154084
- Nor Hadiani, I., Ali, A.M., Aimi, N., Kitajima, M., Takayama, H. & Nordin, H.L. 1997. Anthraquinones from *Morinda elliptica*. *Phytochemistry* 45: 1723-1725. [https://doi.org/10.1016/S0031-9422\(97\)00252-5](https://doi.org/10.1016/S0031-9422(97)00252-5)
- Nualsanit, T., Rojanapanthu, P., Gritsanapan, W., Lee, S.H., Lawson, D. & Baek, S.J. 2012. Damnacanthal, a noni component, exhibits antitumorigenic activity in human colorectal cancer cells. *Journal of Nutritional Biochemistry* 23: 915-923. doi: 10.1016/j.jnutbio.2011.04.017
- Park, C., Shin, H.J., Kim, G.Y., Kwon, T.K., Name, T.J., Kim, S.K., Cheong, J., Choi, I.W. & Choi, Y.H. 2008. Induction of apoptosis by streptochlorin isolated from *Streptomyces* sp. in human leukaemic U937 cells. *Toxicology in Vitro* 22: 1573-1581. doi: 10.1016/j.tiv.2008.06.010
- Parrish, A.B., Freel, C.D. & Kornbluth, S. 2013. Cellular mechanisms controlling caspase activation and function. *Cold Spring Harbor Perspectives in Biology* 5(6): 008672. doi: 10.1101/cshperspect.a008672
- Povea-Cabello, S., Oropesa-Ávila, M., de la Cruz-Ojeda, P., Villanueva-Paz, M., de la Mata, M., Suárez-Rivero, J.M., Álvarez-Córdoba, M., Villalón-García, I., Cotán, D., Ybot-González, P. & Sánchez-Alcázar, J.A. 2017. Dynamic reorganization of the cytoskeleton during apoptosis: The two coffins hypothesis. *International Journal of Molecular Sciences* 18(11): 2393. <https://doi.org/10.3390/ijms18112393>
- Prasad, V., Chandele, A., Jagtap, J.C., Kumar, S. & Shastri, P. 2006. ROS-triggered caspase 2 activation and feedback amplification loop in  $\beta$ -carotene-induced apoptosis. *Free Radical Biology & Medicine* 41: 431-442. doi: 10.1016/j.freeradbiomed.2006.03.009
- Rajendran, M., Inbaraj, J.J., Gandhidasan, R. & Murugesan, R. 2004. Photodynamic action of damnacanthal and nordamnacanthal. *Journal of Photochemistry and Photobiology A: Chemistry* 162: 615-623. [https://doi.org/10.1016/S1010-6030\(03\)00415-5](https://doi.org/10.1016/S1010-6030(03)00415-5)
- Schonthal, A.H., Mueller, S. & Cadenas, E. 2000. Redox regulation of p21, role of reactive oxygen and nitrogen species in cell cycle progression. In *Antioxidant and Redox Regulation*, edited by Sen, C.K., Sies, H. & Baeuerle, P.A. Massachusetts: Academic Press. pp. 311-336.
- Schutte, B., Henfling, M., Kolgen, W., Bouman, M., Meex, S., Leers, M.P.G., Nap, M., Bjorklund, V., Bjorklund, P., Bjorklund, B., Lane, E.B., Omary, M.B., Jornvall, H. & Ramaekers, F.C.S. 2004. Keratin 8/18 breakdown and reorganization during apoptosis. *Experimental Cell Research* 297: 11-26. doi: 10.1016/j.yexcr.2004.02.019
- Shaghayegh, G., Alabsi, A.M., Ali-Saeed, R., Ali, A.M., Vincent-Chong, V.K., Ismail, N.H., Choon, Y.F. & Zain, R.B. 2017. Effects of damnacanthal and nordamnacanthal on proliferation, apoptosis, and migration of oral squamous cell carcinoma cells. *Asian Pacific Journal of Cancer Prevention* 18: 3333-3341. doi: 10.22034/APJCP.2017.18.12.3333
- Shami, A.M.M. 2018. Antibacterial and antioxidant properties of anthraquinones fractions from *Morinda citrifolia* fruit. *Journal of Reports in Pharmaceutical Sciences* 7: 379-388. [https://www.researchgate.net/publication/329487739\\_Antibacterial\\_and\\_Antioxidant\\_Properties\\_of\\_Anthraquinones\\_Fractions\\_from\\_Morinda\\_Citrifolia\\_Fruit](https://www.researchgate.net/publication/329487739_Antibacterial_and_Antioxidant_Properties_of_Anthraquinones_Fractions_from_Morinda_Citrifolia_Fruit) (Accessed on 6 June 2023).

- Shieh, D.E., Chen, Y.Y., Yen, M.H., Chiang, L.C. & Lin, C.C. 2004. Emodin-induced apoptosis through p53-dependent pathway in human hepatoma cells. *Life Sciences* 74: 2279-2290. doi: 10.1016/j.lfs.2003.09.060
- Siegel, R.L., Miller, K.D., Wagle, N.S. & Jemal, A. 2023. Cancer statistics. *A Cancer Journal for Clinicians* 73(1): 17-48. doi:10.3322/caac.21763
- Silva, G.M., Saavedra, V., Ianez, R.C.F., Sousa, E.A., Gomes, N., Kelner, N., Nagai, M.A., Kowalski, L.P., Soares, F.A., Lourenço, S.V. & Coutinho-Camillo, C.M. 2019. Apoptotic signaling in salivary mucoepidermoid carcinoma. *Head and Neck* 41: 2904-2913. doi: 10.1002/hed.25763
- Stennicke, H.R. & Salvesen, G.S. 1998. Properties of the caspases. *Biochimica et Biophysica Acta* 1387: 17-31.
- Su, Y.T., Chang, H.L., Shyue, S.K. & Hsu, S.L. 2005. Emodin induces apoptosis in human lung adenocarcinoma cells through a reactive oxygen species-dependent mitochondrial signaling pathway. *Biochemical Pharmacology* 70: 229-241. doi: 10.1016/j.bcp.2005.04.026
- Tamura, Y., Simizu, S. & Osada, H. 2004. The phosphorylation status and anti-apoptotic activity of Bcl-2 are regulated by ERK and protein phosphatase 2A on the mitochondria. *FEBS Letters* 569: 249-255. doi: 10.1016/j.febslet.2004.06.003
- Tseng, C.J., Wang, Y.J., Liang, Y.C., Jeng, J.H., Lee, W.S., Lin, J.K., Chen, C.H., Liu, I.C. & Ho, Y.S. 2002. Microtubule damaging agents induce apoptosis in HL 60 cells and G2/M cell cycle arrest in HT29 cells. *Toxicology* 175: 123-142. doi: 10.1016/s0300-483x(02)00073-2
- Van Opdenbosch, N. & Lamkanfi, M. 2019. Caspases in cell death, inflammation, and disease. *Immunity* 50(6): 1352-1364. doi: 10.1016/j.immuni.2019.05.020
- Wang, H., Guo, M., Wei, H. & Chen, Y. 2023. Targeting p53 pathways: Mechanisms, structures, and advances in therapy. *Signal Transduction and Targeted Therapy* 8(1): 92. <https://doi.org/10.1038/s41392-023-01347-1>
- Wei, H., Qu, L., Dai, S., Li, Y., Wang, H., Feng, Y., Chen, X., Jiang, L., Guo, M., Li, J., Chen, Z., Chen, L., Zhang, Y. & Chen, Y. 2021. Structural insight into the molecular mechanism of p53-mediated mitochondrial apoptosis. *Nature Communications* 12: 2280. <https://doi.org/10.1038/s41467-021-22655-6>
- World Health Organization (WHO). 2021. Assessing national capacity for the prevention and control of noncommunicable diseases: Report of the 2019 global survey. World Health Organization. <https://apps.who.int/iris/handle/10665/331452>
- Woradulayapinij, W., Pothiluk, A., Nualsanit, T., Yimsoo, T., Yingmema, W., Rojanapanthu, P., Hong, Y., Baek, S.J. & Treesuppharat, W. 2022. Acute oral toxicity of damnacanthol and its anticancer activity against colorectal tumorigenesis. *Toxicology Reports* 9: 1968-1976. doi: 10.1016/j.toxrep.2022.10.015
- Zhivotovsky, B. & Orenius, R. 2005. Caspase-2 function in response to DNA damage. *Biochemical and Biophysical Research Communications* 331: 859-867. doi: 10.1016/j.bbrc.2005.03.191

\*Corresponding author; email: latifahsy@upm.edu.my